
Federation of Experts: Communication Efficient Distributed Inference for Large Language Models

Muhammad Shahir Abdurrahman 
Stanford University
shahir@stanford.edu

Chun Deng
Stanford University
dengchun@stanford.edu

Azalia Mirhoseini
Stanford University
azalia@stanford.edu

Philip Levis
Stanford University
plevis@stanford.edu

Abstract

Mixture of experts has emerged as the primary mechanism for making Large Language Models (LLMs) computationally efficient. However, in distributed settings, communicating token embeddings between experts is a significant bottleneck.

We present the novel Federation of Experts (FoE) architecture. FoE restructures the MoE block of a transformer layer into multiple MoE clusters. Each cluster is responsible for only one of the KV heads and expert parallelism is applied between those experts. Between clusters, a sum synchronizes the post-attention residuals, which then drives routing and dispatch for the next MoE block. In a single-node setting, FoE completely eliminates all-to-all communication as all experts within a group are contained on the same GPU. In multi-node settings, FoE confines all-to-all communication to the intra-node fabric, thus significantly reducing communication overhead.

An implementation of FoE finds that on LongBench, FoE significantly improves inference throughput and latency in both single-node and multi-node settings, reducing the end-to-end forward-pass latency by up to $5.2\times$, TTFT by $3.62\times$, and TBT by $1.95\times$. It does so while achieving comparable generation quality to a mixture of experts model of the same size and training configuration.

1 Introduction

Large Language Models (LLMs) are the backbone for many modern AI applications. Driven by the transformer architecture [23], these models consistently improve as parameter counts increase [3, 22]. However, computation scales proportionally with parameters, imposing limits on both training efficiency and inference deployment.

Mixture-of-Experts (MoE) architectures are a widely adopted paradigm [20] to mitigate the computational costs of scaling dense transformer models. MoE models sparsely activate only a subset of experts in the feed-forward networks for each token, decoupling the total parameter count from the active parameters per token. MoE scaling has been validated to hundreds of billions of parameters [6, 11]. These compute efficiency gains, however, introduce a new bottleneck in distributed settings: the sparse routing mechanism in expert parallelism. When a token is assigned to an expert residing on a different GPU, it must be dispatched across the network, relying on expensive bandwidth-bounded communication primitives. This worsens with the number of GPUs, and accounts for 68%+ of end-to-end latency [1]. For example, in DeepSeek production deployments for their V3/R1 models, 256 experts are distributed across 18 nodes for decode and 4 nodes for prefill, with 8 GPUs per node, in order to achieve higher throughput with larger batch sizes [4]. With expansive intra-node GPU interconnect fabrics and intra-node networking becoming increasingly common, the communication overhead is a very important problem to address.

When exploring communication in the MoE architecture, we find that the required all-to-all primitive for standard expert parallelism across a cluster is a major bottleneck for distributed inference, as illustrated in Figure 1.

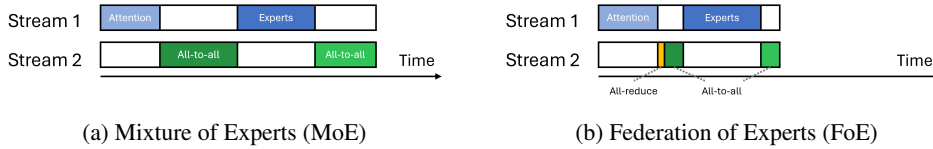


Figure 1: Timing diagrams comparing standard MoE and FoE. FoE confines all-to-all communication into localized clusters, mitigating the network bottleneck in distributed settings.

In multi-node deployments, the problem becomes more pronounced, as intra-node NVLink delivers up to 900 GB/s [18], while inter-node InfiniBand caps at 400 Gb/s per link [24], a gap of roughly $18\times$. Improvements must focus on maximizing the Local Activation Rate (LAR) - the proportion of expert selections that are resolved locally without network transfer. In standard MoE, as the hardware cluster size grows, the LAR falls, forcing the majority of tokens to leave their resident GPUs and incur substantial network latencies.

This paper introduces the Federation of Experts (FoE) architecture to reduce this inter-expert communication bottleneck. FoE restructures the attention and MoE FFN layers into H independent MoE groups. Here k denotes the top- k experts selected per token per layer, and H denotes the number of expert groups. Each group owns $1/H$ of the KV heads and $1/H$ of the experts, and runs on its own subset of GPUs. Instead of performing a single global top- k routing over all experts, FoE uses per-group routing: each token selects k/H experts exclusively inside every group. Post-attention residuals from the H groups are synchronized using a comparatively lightweight cross-group all-reduce to form the shared routing input. By ensuring that dispatch and combine operations are strictly contained within each group, FoE keeps the expensive k -proportional all-to-all traffic localized to the expert group, structurally enforces uniform load distribution across GPUs between groups, and minimizes expensive network traffic over the slower cross-node InfiniBand fabric.

This paper makes three contributions:

1. We describe the Federation of Experts architecture, which partitions experts and KV heads into isolated clusters, restructuring expert parallelism to significantly limit communication to guarantee even distributed load across GPUs on single node deployments and substantially improving inference latency and throughput without sacrificing generation quality.
2. We show how FoE obtains an order-of-magnitude reduction in communication for both single-node and multi-node inference.
3. We experimentally demonstrate that on the LongBench dataset [2], this improvement reduces end-to-end forward-pass latency by up to $5.2\times$, time-to-first-token (TTFT) by $3.62\times$, and time-between-tokens (TBT) by $1.95\times$, while achieving comparable generation quality to a mixture of experts model of the same size and training configuration.

2 Background

Mixture-of-Experts. Mixture of Experts (MoE) models [20] were motivated by the need to increase the total number of parameters in a model without a proportional increase in computational requirements. In a traditional dense model, all parameters are activated for each input token, which leads to a linear or even superlinear scaling of computational costs as the model size increases. In contrast, an MoE model consists of multiple expert networks within each transformer block, and only a subset of these experts are activated for each input token [14, 6]. This allows for a significant reduction in the active parameters per token, enabling more efficient use of computational resources, and has been adopted by many recent open production-scale LLMs [11, 4, 17].

The FFN block of a transformer layer is typically the largest component in terms of parameters, and thus is the primary target for MoE architectures. In an MoE model, the dense FFN block is replaced with multiple expert FFN blocks, and a gate network is used to produce a routing policy that assigns each input token to a subset of these experts. In a token-choice MoE FFN block [20, 14] (the most common and standard MoE architecture) the gate network produces a weight distribution over the

experts for each input token. For each individual token, experts with the top- k weights are selected and the outputs of the selected experts are combined in a weighted sum to produce the final output for the token. This results in activation of only the parameters in the top- k experts, thus significantly reducing the computational requirements for each token compared to a dense model with the same number of total parameters in the FFN block [20].

MoE Inference Systems and Parallelism. Integrated serving engines such as DeepSpeed-MII [10], vLLM [13], and SGLang [28] optimize LLM inference through continuous batching, high-performance kernels, and other graph-level optimization techniques such as pipeline parallelism. On top of these optimizations, specialized engines for Mixture of Experts models such as DeepSpeed-MoE [19, 21], and now vLLM/SGLang as well, rely heavily on Expert Parallelism (EP). In an EP setup, experts are scattered across multiple devices. EP requires that token activations be sent to the physical device holding the selected expert (dispatch) through all-to-all communication. Naively, as cluster sizes scale up in a throughput bottlenecked inference environment, the probability of an expert residing on the same device where the token originates collapses, making communication overhead a growing and significant bottleneck, accounting for 47% to 68% of the inference time [26, 1].

Expert Parallelism Optimizations. Real-world MoE deployment frequently suffers from unbalanced routing and network-bound hot-spotting. To mitigate computational inefficiencies, prior work utilizes expert replication and load balancing [15, 4]. To mask the steep all-to-all communication overhead, systems-level optimizations aggressively pipeline execution: COMET [26] applies fine-grained computation-communication overlapping via task rescheduling, FlashMoE [1] fuses the distributed MoE operator to eliminate launch overhead, and DeepEP [27] leverages pure RDMA overlapping.

At the same time, scheduling frameworks exploit expert affinity to minimize cross-node routing. Sem-MoE [16] and GRACE-MoE [8] proactively colocate experts and their activating tokens to reduce communication. To harness structural predictability, ExFlow [25] and MoETuner [7] exploit predictable inter-layer routing dependencies via integer programming to optimize static expert-to-GPU assignments.

Other methods restructure the MoE architecture to bypass standard communication limits. Big-Mac [12] projects communication into a lower dimension using a descend-communicate-ascend mechanism, while LatentMoE [5] projects MoE routing and computation into a compact latent space.

While these scheduling, kernel fusion, and architectural projection methods succeed at optimizing the global dispatch process, they still fundamentally operate within a traditional unified Expert Parallel (EP) group, leaving them bounded by unavoidable inter-node communication limits. Instead, FoE takes a structural approach: by restructuring the global routing operation into disjoint, balanced expert groups, FoE natively confines traffic topologies. This guarantees a balanced, high Local Activation Rate (LAR) across all cluster nodes and sidesteps the global all-to-all inter-node bottleneck without complex dynamic scheduling or low-dimensional approximations.

3 Federation of Experts

When experts are distributed across GPUs, the fundamental communication primitive for sending tokens to and from their selected experts is all-to-all. This is because a token’s selected experts can reside on any of the G GPUs, but the GPU holding its input and KV cache may not hold those experts. This mismatch cannot be avoided without disconnecting the attention computation from

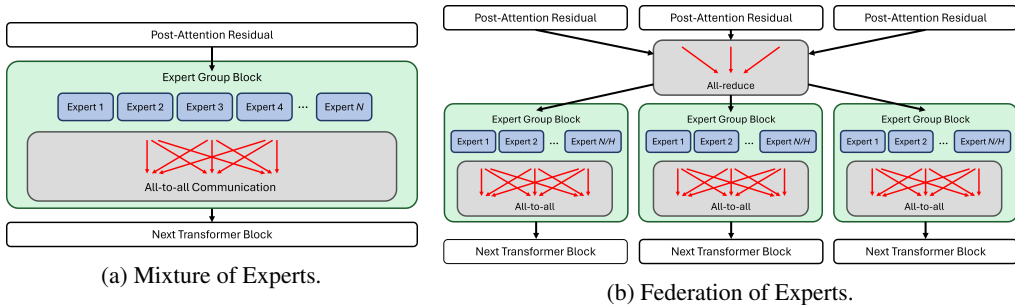


Figure 2: Comparison in expert communication between MoE and FoE.

the FFN computation, which would significantly degrade model quality. All-to-all communication is expensive, and as cluster sizes and batch sizes scale up in a throughput-bottlenecked inference environment, the proportion of end-to-end time devoted to communication grows significantly.

Federation of Experts (FoE) addresses this bottleneck structurally by increasing the number of GPUs where a token’s attention computation is performed. By doing this, fewer tokens need to be sent off-GPU for their selected experts, and more can be resolved locally without all-to-all. FoE achieves this by replacing the single expert-parallel MoE block in each transformer layer with H independent MoE clusters, which we call *expert groups*. Each group owns $1/H$ of the KV heads, $1/H$ of the experts, and $1/H$ of the GPUs. Routing is per-group: each token selects k/H experts from each group rather than k from the full pool, so every group contributes to every token at every layer. The H groups synchronize once per layer through a cross-group sum of their post-attention residuals; dispatch and combine all-to-alls are strictly intra-group. Figure 2 contrasts this with MoE: one global all-to-all over G GPUs is replaced by H disjoint intra-group all-to-alls (each over G/H GPUs) plus a much smaller cross-group all-reduce.

The central quantity for analysis is the local activation rate ρ , the fraction of expert selections resolved on the token’s local GPUs (and which therefore require no all-to-all). Notation used throughout is summarized in Table 1. By splitting the KV cache across H expert groups, FoE improves the expert-GPU assignment problem structurally, by increasing the minimum probability that a token’s selected experts are co-located with its attention computation. While many prior works attempt to analyze historical expert routing patterns and speculatively compute a better expert-GPU assignment to thereby increase ρ , FoE guarantees a much higher local activation rate (LAR) by design.

In a standard MoE, the feasibility condition for full local resolution is $k \leq E/G$. For fine-grained MoE models with high k deployed across large G , E/G becomes small and this condition fails for most tokens, forcing them through the all-to-all for most of their k selections. FoE relaxes the condition by $H\times$: the per-group analogue is $k/H \leq E/G$, structurally raising ρ and reducing all-to-all volume in any deployment. On multi-node deployments the benefit compounds: every intra-group all-to-all stays within a single node, significantly reducing the expensive cross-node InfiniBand/Ethernet traffic that MoE’s global dispatch incurs.

Symbol	Meaning
G	Total GPUs in the deployment
$N, G_n = G/N$	Number of nodes, GPUs per node
$H = n_{kv}$	Expert groups in FoE (set equal to the model’s KV-head count)
L, E, k	MoE layers, total routed experts, top- k per token (k a multiple of H)
S, d	Tokens per batch, hidden dimension
i, h, l, e	Token, group, layer, expert indices
$x[i] / x[h, i]$	Hidden state at a layer boundary (MoE / per-group in FoE)
$r[i] / r[h, i]$	Post-attention residual (MoE / per-group in FoE)
$r_{\text{full}}[i]$	Cross-group averaged residual: $\frac{1}{H} \sum_h r[h, i]$
$g[i] \in \mathbb{R}^E$	Router scores over all E experts
\mathcal{E}_h	Expert index block owned by group h : $\{h \cdot E/H, \dots, (h+1) \cdot E/H - 1\}$
$\mathcal{I}_h[i], w_h[i]$	Top- k/H expert indices and routing weights for group h , token i
ρ	Local activation rate (fraction of expert selections resolved on-GPU)
$V^{\text{A2A}}, V^{\text{AR}}$	Per-layer all-to-all and all-reduce communication volumes (in units of $S \cdot d$)
$B_{\text{intra}}, B_{\text{inter}}$	Intra-node (NVLink/NVSwitch/PCIe) and inter-node (InfiniBand/Ethernet) bandwidth
$r = B_{\text{intra}}/B_{\text{inter}}$	Intra/inter-node bandwidth ratio ($r \approx 15\text{--}20$ on H100-class hardware)
T	Bandwidth-weighted per-layer communication time

Table 1: Notation used throughout the Design section.

3.1 Architecture Formulation

This section presents the architectural formulation of Federation of Experts (FoE) and contrasts it with the traditional Mixture of Experts (MoE). The key difference is that FoE maintains separate representations for each expert group, which allows it to confine routing and MoE updates to per-group subsets of experts and GPUs. While a MoE keeps a single representation $x \in \mathbb{R}^{S \times d}$ at every layer boundary, FoE carries an H -fold representation $x \in \mathbb{R}^{H \times S \times d}$ between intermediate layers (one separate input per expert group), collapsing to $\mathbb{R}^{S \times d}$ only at the initial input embedding and after the

final MoE layer’s cross-group average. Table 2 compares the two architectures step-by-step on an intermediate MoE layer.

	Mixture of Experts $x \in \mathbb{R}^{S \times d}$	Federation of Experts $x \in \mathbb{R}^{H \times S \times d}$
Attn. residual	$r[i] = x[i] + \text{Attn}(x)[i]$	$r[h, i] = x[h, i] + \text{Attn}_h(x[h, :])[i]$
Cross-group avg.	—	$r_{\text{full}}[i] = \frac{1}{H} \sum_h r[h, i]$
Routing	$\mathcal{I}[i], w[i] = \text{Router}(r[i])$	$\mathcal{I}_h[i], w_h[i] = \text{Router}(r_{\text{full}}[i])$
MoE update	$x'[i] = r[i] + \sum_{e \in \mathcal{I}[i]} w[i, e] \text{FFN}_e(r[i])$	$x'[h, i] = r_{\text{full}}[i] + \sum_{e \in \mathcal{I}_h[i]} w_h[i, e] \text{FFN}_e(r_{\text{full}}[i])$

Table 2: Per-layer compute for MoE and FoE on an intermediate layer ($1 < l < L$). All equations are per token $i \in [S]$. The first and last MoE layers in FoE differ only at the input/output boundaries (see text).

Layer boundaries. The first MoE layer ($l = 1$) receives the embedding $x^{(1)} \in \mathbb{R}^{S \times d}$ (no per-group dimension), runs a single shared attention to produce one residual r , and then applies the routing and MoE-update with r in place of r_{full} to produce $x^{(2)} \in \mathbb{R}^{H \times S \times d}$. The last MoE layer ($l = L$) is identical to the intermediate case but appends a final cross-group average $x^{(L+1)}[i] = \frac{1}{H} \sum_h x'[h, i]$ to project back to a single $\mathbb{R}^{S \times d}$ representation before the final linear token head.

Routing. Each expert group h owns the contiguous block of experts $\mathcal{E}_h = \{h \cdot E/H, \dots, (h+1) \cdot E/H - 1\}$. The router produces a single global score vector, and each group independently selects its top- k/H experts from within its own expert group:

$$g[i] = \text{Router}(r_{\text{full}}[i]) \in \mathbb{R}^E, \quad \mathcal{I}_h[i], w_h[i] = \text{TopK}(g[i], k/H) \quad \forall h \in [H], i \in [S].$$

$e \in \mathcal{E}_h$

3.2 Communication Analysis

This section analyzes the communication volume and latency of a FoE architecture compared to a standard MoE architecture, decomposing traffic into intra-node and inter-node components. A central quantity for the analysis is the local activation rate ρ , which we define as the fraction of expert selections resolved on the token’s local GPUs (and which therefore require no all-to-all). Under balanced routing, effective per-layer A2A volume is $2k(1 - \rho) \cdot S \cdot d$. Mixture of Experts achieves $\rho_{\text{moe}} = 1/G$, while Federation of Experts achieves $\rho_{\text{foe}} = \min(H/G, 1)$, because each group only needs to resolve k/H selections per token.

Each experts layer has dispatch and combine all-to-alls (identical in volume), and for FoE, one additional cross-group all-reduce. The all-reduce runs across $\min(G, H)$ participants — physically H -way when $G \geq H$ (each group occupies its own GPU or set of GPUs), and G -way when $G < H$ (multiple groups sharing a GPU combine partials locally before the network hop). Substituting $\rho_{\text{moe}} = 1/G$ and $\rho_{\text{foe}} = \min(H/G, 1)$ into the effective A2A volume $2k(1 - \rho)$ gives:

$$V_{\text{moe}}^{\text{A2A}} = 2k \cdot \frac{G-1}{G}, \quad V_{\text{foe}}^{\text{A2A}} = 2k \cdot \frac{\max(G-H, 0)}{G}, \quad V_{\text{foe}}^{\text{AR}} = \frac{2(\min(G, H) - 1)}{\min(G, H)}.$$

We report communication volumes as aggregate egress across all participating GPUs in units of $S \cdot d$.

Single-node deployment ($N = 1$). In almost all single-node settings $G \leq H$ because n_{kv} is typically 8 or more in modern production models and almost no single-node deployments have more than 8 GPUs. We therefore restrict attention to the $G \leq H$ regime for single-node, under which the FoE A2A term vanishes ($\rho = 1$) and only the cross-group all-reduce (of volume $2(G - 1)/G$) remains.

Architecture	Per-layer volume (intra-node)
Mixture of Experts	$2k \cdot \frac{G-1}{G}$
Federation of Experts	$2 \cdot \frac{G-1}{G}$

Table 3: Per-layer communication volume (units of $S \cdot d$) for a single-node deployment ($N = 1$, $G \leq H$). FoE eliminates the k -proportional A2A term, reducing volume by exactly $k \times$.

The communication volume ratio collapses to $V_{\text{moe}}/V_{\text{foe}} = k$, meaning communication reduction on a single node is exactly $k \times$ for any $G \leq H$, whether the node matches the model exactly ($G = H$) or

is under-provisioned relative to the model ($G < H$). This is particularly valuable for non-production scale deployments (edge boxes, workstations, single-node inference) where MoE’s $(G - 1)/G$ factor pushes it close to the full $2k$ naive cost.

Multi-node deployment ($1 < N \leq H$). For FoE, experts are assigned to GPUs such that each expert group spans at most one node. This way dispatch and combine all-to-alls are intra-node regardless of N . When $N < H$, multiple groups share a node (each group gets an equal subset of the GPUs). MoE, in contrast, runs a single EP group across all N nodes, so under balanced routing a fraction $(N - 1)/N$ of its A2A crosses node boundaries. The same fraction applies to the FoE all-reduce when the ring is ordered so that same-node groups are consecutive. Multi-node deployments have $G \geq H$, so the FoE all-reduce term takes the $2(H - 1)/H$ form, bounding inter-node volume above by ≈ 2 regardless of k ; MoE’s inter-node volume, by contrast, grows linearly in k .

Raw volumes understate the actual cost difference because inter-node bandwidth is typically much lower than intra-node. Let $r = B_{\text{intra}}/B_{\text{inter}}$ (on H100-class hardware, $r \approx 15$ to 20); weighting inter-node volume by r gives total per-layer time. Table 4 summarizes both raw aggregate volumes and bandwidth-weighted total time.

	Mixture of Experts	Federation of Experts
Intra-node	$\frac{2k}{N} \cdot \frac{G-1}{G}$	$2k \cdot \frac{G-H}{G} + \frac{1}{N} \cdot \frac{2(H-1)}{H}$
Inter-node	$\frac{2k(N-1)}{N} \cdot \frac{G-1}{G}$	$\frac{N-1}{N} \cdot \frac{2(H-1)}{H}$
Total time	$\frac{2k}{N} \cdot \frac{G-1}{G} \cdot [1 + r(N-1)]$	$2k \cdot \frac{G-H}{G} + \frac{2(H-1)}{H} \cdot \frac{1+r(N-1)}{N}$

Table 4: Per-layer communication cost in a multi-node deployment ($N \leq H$), in units of $S \cdot d$. The first two rows give raw aggregate volumes; the last row weights inter-node by $r = B_{\text{intra}}/B_{\text{inter}}$ (typically 15–20 on H100-class hardware) so it predicts wall-clock latency.

The total-time ratio collapses to a clean asymptote:

$$\frac{T_{\text{moe}}}{T_{\text{foe}}} = \frac{\frac{2k}{N} \cdot \frac{G-1}{G} \cdot [1 + r(N-1)]}{2k \cdot \frac{G-H}{G} + \frac{2(H-1)}{H} \cdot \frac{1+r(N-1)}{N}} \rightarrow \frac{kHr}{kH + r(H-1)} \quad (N \rightarrow \infty, G = G_n N).$$

For $k = 8, H = 8, r = 20$ the asymptote is $\approx 6.3\times$, which is within $\sim 5\%$ of the actual formula for $N \geq 2$.

4 Experiments

4.1 Experimental Setup

Hardware. We evaluate performance across two deployment regimes: a single-node configuration utilizing an 8-GPU server equipped with NVIDIA H100 (SXM, HBM3) GPUs with 80GB of VRAM each, and a multi-node configuration consisting of two identical 8-GPU servers connected via InfiniBand. Both servers feature dual-socket Intel Xeon CPUs and 2TB of DDR5 memory.

Inference Framework. To ensure a rigorous comparison, we implement both Expert Parallelism (EP) and federation parallelism within **FlexServe**, our MoE inference engine based on FlexAttention, which we will open source. Standard expert parallelism distributes experts across all GPUs, requiring tokens to route globally through all-to-alls. Federation parallelism divides GPUs and experts into groups, requiring a token to route to every group during inference. To match state-of-the-art system designs, FlexServe integrates many SoTA training and inference techniques, including PagedAttention, chunked prefill/piggyback serving, data-parallelism, pipeline parallelism, and activation checkpointing [13, 28]. Implementing the standard EP directly within FlexServe properly isolates our architectural communication gains from framework-level engineering disparities.

Model Pre-Training. Because FoE modifies the underlying architecture (e.g., routing modifications, partitioning of W_Q projections, etc.), standard open-source MoE checkpoints cannot be evaluated off-the-shelf. To empirically validate that restricted routing does not degrade convergence, we pretrain two OLMoE-like models from scratch alongside equivalently-sized MoE baselines. Figure 3 visualizes the cross-entropy training loss for both configurations, confirming that the localized routing constraint of FoE maintains the same convergence trajectory as MoE. We provide additional model and training details in Appendix A.

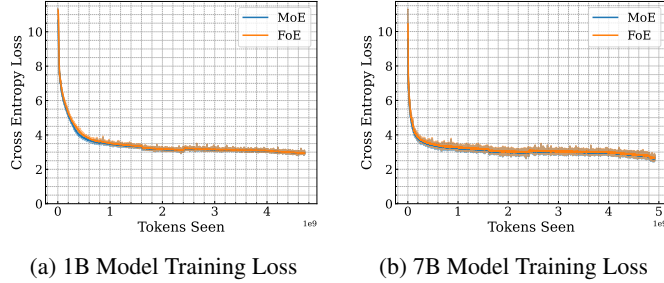


Figure 3: Cross-entropy (CE) loss curves at the end of pre-training. The 1B FoE and MoE curves are indistinguishable at the end of Chinchilla-level training; the 7B model is trained to $5\times$ its active parameter count [9, 17].

4.2 Evaluation Baselines and Metrics

Baselines. Our primary baseline is expert parallelism (EP) utilizing global all-to-all dispatch as done in SoTA inference engines like vLLM and SGLang. By executing this baseline within FlexServe, we emulate the architectural behavior of vLLM and SGLang without confounding framework overhead differences. We explicitly exclude predictive token-expert scheduling frameworks (e.g., MoETuner [7], Sem-MoE [16]) in end-to-end latency evaluations, as FoE’s architectural confinement natively enforces perfect per-GPU balancing and expert-gpu colocation, and those improvements are orthogonal. However, we do cross-compare against these methods on Local Activation Rate (LAR) to contrast system approximations against structural guarantees.

Metrics. Unlike many prior works which rely on synthetic evaluations, we model real-world request distributions using a Poisson arrival process on LongBench [2]. We separate our latency evaluation into prefill and decode stages using the following metrics: Time to First Token (TTFT, time elapsed between request arrival and the generation of the first token), Time Between Token (TBT, average time elapsed per generated token during the decode phase), and End-to-End (E2E) Latency (total completion time for a request sequence).

4.3 End-to-End Inference Performance

We measure Time to First Token (TTFT) and Time Between Tokens (TBT) to capture inference performance. Table 5 shows data for our single-node experiments including mean, p50, and p99 values across varying request arrival scales (Poisson distribution). FoE substantially reduces TTFT by up to $3.1\times$ on average and bounds outlier tails significantly better than MoE. This emphasizes FoE’s inherent advantage in managing tail latencies by enforcing localized load-balancing guarantees without waiting on global stragglers (see section 4.5).

Scale	Architecture	TTFT (s)			TBT (s)			E2E (s)		
		Mean	p50	p99	Mean	p50	p99	Mean	p50	p99
0.5	MoE	3.710	3.623	6.437	0.780	0.783	0.979	202.7	203.1	253.3
	FoE	1.394	1.213	3.528	0.566	0.596	0.639	145.7	153.8	164.3
	<i>Speedup</i>	$2.66\times$	$2.99\times$	$1.82\times$	$1.38\times$	$1.31\times$	$1.53\times$	$1.39\times$	$1.32\times$	$1.54\times$
0.75	MoE	3.233	3.147	5.856	0.841	0.869	1.033	217.7	225.2	266.6
	FoE	1.041	0.979	2.116	0.458	0.458	0.502	117.9	117.8	129.0
	<i>Speedup</i>	$3.11\times$	$3.21\times$	$2.77\times$	$1.83\times$	$1.90\times$	$2.06\times$	$1.85\times$	$1.91\times$	$2.07\times$
1.5	MoE	2.264	2.118	5.128	0.371	0.360	0.558	96.9	93.8	146.7
	FoE	0.790	0.744	1.627	0.334	0.333	0.365	86.0	85.6	94.1
	<i>Speedup</i>	$2.87\times$	$2.85\times$	$3.15\times$	$1.11\times$	$1.08\times$	$1.53\times$	$1.13\times$	$1.09\times$	$1.56\times$

Table 5: Single-Node inference performance metrics across various Poisson request arrival scales. Time-to-First-Token (TTFT), Time-Between-Tokens (TBT), and End-to-End Latency (E2E).

4.4 Scaling to Multi-Node Distributed Inference

Modern deployments often exceed the boundaries of a single node. In these configurations, all-to-all communication requires off-node transfer via slower inter-connects like InfiniBand rather than

high-throughput NVLink. Table 6 characterizes inference performance on a multi-node configuration consisting of two identical 8-GPU servers.

FoE scales gracefully to larger hardware deployments, and as expected from its design, sees a *larger* relative improvement moving from single-node to multi-node than the baseline MoE. For instance, at an arrival scale of 0.5, FoE’s TTFT speedup over standard MoE increases from $2.66\times$ in the single node setup to $3.44\times$ in the multi-node distributed regime. This occurs because the baseline MoE forces token dispatch across the entire combined hardware topology layer, incurring severe interconnect penalties. In contrast, FoE structurally confines all-to-all dispatch/combine strictly within localized expert groups, shielding the architecture from the bottleneck of slow inter-node network fabrics. Tail latencies exhibit similar multi-node advantages; at 0.5 scale, average FoE p99 TTFT stays low at 2.575s vs standard MoE’s inflated 7.066s.

Scale	Architecture	TTFT (s)			TBT (s)			E2E (s)		
		Mean	p50	p99	Mean	p50	p99	Mean	p50	p99
0.5	MoE	3.883	3.708	7.066	0.736	0.739	0.940	191.5	192.5	242.6
	FoE	1.128	1.038	2.575	0.543	0.557	0.601	139.5	143.5	154.4
	<i>Speedup</i>	$3.44\times$	$3.57\times$	$2.74\times$	$1.36\times$	$1.33\times$	$1.57\times$	$1.37\times$	$1.34\times$	$1.57\times$
0.75	MoE	3.403	3.261	6.218	0.876	0.895	1.120	226.7	232.1	288.7
	FoE	0.939	0.908	1.679	0.449	0.446	0.495	115.4	115.2	127.3
	<i>Speedup</i>	$3.62\times$	$3.59\times$	$3.70\times$	$1.95\times$	$2.01\times$	$2.26\times$	$1.96\times$	$2.02\times$	$2.27\times$

Table 6: Multi-Node inference performance metrics on two identical 8-GPU servers connected via InfiniBand. Both Time-to-First-Token (TTFT) and tail distributions scale efficiently due to localized routing shielding traffic from slow inter-node networks.

4.5 Local Activation Rate and GPU Load Imbalance

A critical factor driving the communication efficiency of FoE is its ability to maximize the Local Activation Rate (LAR) while simultaneously maintaining perfect load balancing. As described before, LAR measures the proportion of token-expert assignments that are resolved locally i.e., where the assigned expert resides on the same GPU as the token.

In Figure 4(a), we compare the LAR of our FoE architecture against prior state-of-the-art predictive and balancing frameworks (Sem-MoE, MoETuner, and ExFlow) at an Expert Parallel (EP) size of 8. Because FoE structurally confines routing within isolated expert groups (in our single-node configuration of 8 GPUs, each group is self-contained), it inherently achieves an LAR of 1.0 (100%). In contrast, heuristic-based proxy methods suffer from structural degradation as EP size scales; at EP=8, Sem-MoE achieves an LAR of 0.39, ExFlow achieves 0.21, and MoETuner drops to 0.12.

Simultaneously, traditional MoE systems relying on global all-to-all routing frequently suffer from acute token processing imbalances across GPUs. We define this GPU load discrepancy as the ratio between the maximum and median number of tokens routed to a GPU during inference. Our execution traces show that standard MoE suffers an average load discrepancy of $1.64\times$, meaning the straggler GPU handles 64% more tokens than the median GPU in a given forward pass. Because standard expert parallelism synchronizes at a global all-to-all, every GPU must wait for the slowest straggler.

Because FoE routes every token to every expert group, all expert groups receive the same number of tokens. In a single-node setting, this means every GPU receives the same number of tokens, making the load perfectly balanced by design. Figure 4b contrasts the GPU load discrepancy of standard Expert Parallelism (EP) against FoE and optimized baselines (values for MoETuner and Sem-MoE are taken directly from their respective publications). FoE achieves a perfect structural GPU load-balance rate of 1.0. The performance gains observed in our single-node and multi-node setups can thus be attributed to reducing this dual bottleneck: minimizing off-GPU/off-node communication (LAR = 1.0), coupled with the removal of strict synchronization barriers caused by stragglers.

4.6 Generation Quality

Table 7 confirms that structurally separating experts into subgroups does not significantly degrade model quality. We compare models directly pre-trained from scratch, demonstrating that the 7B and 1B FoE models achieve zero-shot accuracy strictly comparable to their equivalently-sized MoE

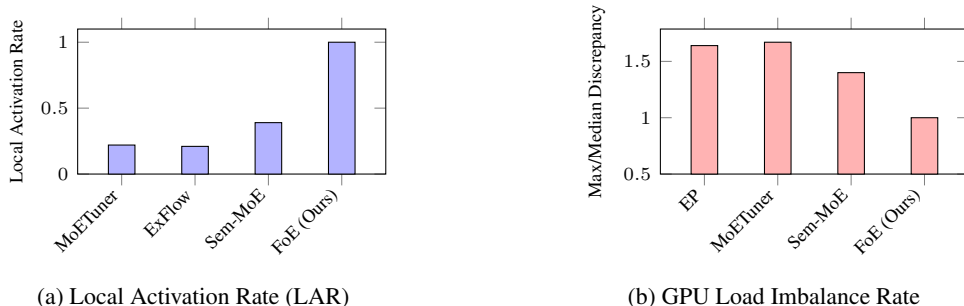


Figure 4: Side-by-side assessment of Structural Efficiency at Expert Parallel (EP) size = 8. (a) FoE structurally guarantees all tokens are processed locally, achieving a perfect LAR of 1.0. (b) Comparison of GPU load discrepancy (max/median token assignments), with values for MoETuner and Sem-MoE sourced from their papers, highlighting FoE’s perfect load balancing.

baselines. These results demonstrate that FoE’s communication savings do not come at the expense of model quality, and are within range of typical training seed variance.

Model Variant	ARC-Easy	BoolQ	COPA	HellaSwag	PIQA	SciQ
MoE (7B)	59.6%	60.4%	65.0%	33.7%	66.9%	80.0%
FoE (7B)	58.2%	60.9%	66.0%	33.1%	66.6%	80.0%
MoE (1B)	53.5%	57.7%	62.0%	30.9%	63.9%	77.7%
FoE (1B)	52.7%	61.4%	61.0%	30.1%	63.8%	74.6%

Table 7: Zero-shot reasoning accuracy on diverse evaluation benchmarks.

5 Limitations

While FoE significantly reduces communication overhead, it introduces additional complexity in model architecture and training. While we show experimentally that FoE models trains to similar performance as traditional MoE Models with identical training hyperparameters, the partitioning of experts and KV heads into isolated groups may require careful tuning of hyperparameters achieve optimal model performance.

FoE’s benefits only apply to distributed deployments. On a single GPU there is no all-to-all to eliminate, and the cross-group all-reduce becomes additional overhead with no offsetting savings. In multi-node deployments with highly asymmetric intra-/inter-node bandwidth, placement of expert groups across nodes affects how much traffic stays intra-node; our evaluation assumes a homogeneous topology, and skewed setups may require placement-aware tuning to fully realize FoE’s benefits.

Finally, our empirical evaluation covers two model sizes (1B and 7B) and two hardware configurations (a single $8 \times H100$ node and a two-node InfiniBand cluster). Training and testing on larger models and longer datasets requires further financial resources.

6 Conclusion

We present Federation of Experts (FoE), a novel architectural reformulation of Mixture-of-Experts that partitions each transformer layer into independent expert groups. This structural modification replaces the global all-to-all of expert parallelism with multiple smaller intra-group all-to-alls plus a much cheaper cross-group all-reduce. This guarantees that more tokens are resolved on the local GPU, leading to a significant reduction in communication overhead. Empirically, FoE delivers up to a $5.2 \times$ end-to-end forward-pass speedup, $3.62 \times$ lower TTFT, and $1.95 \times$ lower TBT, while matching the baseline MoE on cross-entropy loss and zero-shot reasoning. The benefit compounds on multi-node deployments because intra-group all-to-alls remain on the intra-node fabric, while the less expensive reduce communication is placed on the inter-node networking. FoE demonstrates significant improvements in MoE efficiency and scalability, that is orthogonal to existing placement, scheduling, and prefetching optimizations, all of which can still apply on top of FoE.

References

- [1] Osayamen Jonathan Aimuyo, Byungsoo Oh, and Rachee Singh. Flashmoe: Fast distributed moe in a single kernel, 2025. URL <https://arxiv.org/abs/2506.04667>.
- [2] Yushi Bai, Xin Lv, Jiajie Zhang, Hongchang Lyu, Jiankai Tang, Zhidian Huang, Zhengxiao Du, Xiao Liu, Aohan Zeng, Lei Hou, Yuxiao Dong, Jie Tang, and Juanzi Li. Longbench: A bilingual, multitask benchmark for long context understanding, 2024. URL <https://arxiv.org/abs/2308.14508>.
- [3] Tom B. Brown, Benjamin Mann, Nick Ryder, Melanie Subbiah, Jared Kaplan, Prafulla Dhariwal, Arvind Neelakantan, Pranav Shyam, Girish Sastry, Amanda Askell, Sandhini Agarwal, Ariel Herbert-Voss, Gretchen Krueger, Tom Henighan, Rewon Child, Aditya Ramesh, Daniel M. Ziegler, Jeffrey Wu, Clemens Winter, Christopher Hesse, Mark Chen, Eric Sigler, Mateusz Litwin, Scott Gray, Benjamin Chess, Jack Clark, Christopher Berner, Sam McCandlish, Alec Radford, Ilya Sutskever, and Dario Amodei. Language models are few-shot learners, 2020. URL <https://arxiv.org/abs/2005.14165>.
- [4] DeepSeek-AI, Aixin Liu, Bei Feng, Bing Xue, Bingxuan Wang, Bochao Wu, Chengda Lu, Chenggang Zhao, Chengqi Deng, Chenyu Zhang, Chong Ruan, Damai Dai, Daya Guo, Dejian Yang, Deli Chen, Dongjie Ji, Erhang Li, Fangyun Lin, Fucong Dai, Fuli Luo, Guangbo Hao, Guanting Chen, Guowei Li, H. Zhang, Han Bao, Hanwei Xu, Haocheng Wang, Haowei Zhang, Honghui Ding, Huajian Xin, Huazuo Gao, Hui Li, Hui Qu, J. L. Cai, Jian Liang, Jianzhong Guo, Jiaqi Ni, Jiashi Li, Jiawei Wang, Jin Chen, Jingchang Chen, Jingyang Yuan, Junjie Qiu, Junlong Li, Junxiao Song, Kai Dong, Kai Hu, Kaige Gao, Kang Guan, Kexin Huang, Kuai Yu, Lean Wang, Lecong Zhang, Lei Xu, Leyi Xia, Liang Zhao, Litong Wang, Liyue Zhang, Meng Li, Miaojun Wang, Mingchuan Zhang, Minghua Zhang, Minghui Tang, Mingming Li, Ning Tian, Panpan Huang, Peiyi Wang, Peng Zhang, Qiancheng Wang, Qihao Zhu, Qinyu Chen, Qiushi Du, R. J. Chen, R. L. Jin, Ruiqi Ge, Ruisong Zhang, Ruizhe Pan, Runji Wang, Runxin Xu, Ruoyu Zhang, Ruyi Chen, S. S. Li, Shanghao Lu, Shangyan Zhou, Shanhuang Chen, Shaoqing Wu, Shengfeng Ye, Shengfeng Ye, Shirong Ma, Shiyu Wang, Shuang Zhou, Shuiping Yu, Shunfeng Zhou, Shuting Pan, T. Wang, Tao Yun, Tian Pei, Tianyu Sun, W. L. Xiao, Wangding Zeng, Wanbiao Zhao, Wei An, Wen Liu, Wenfeng Liang, Wenjun Gao, Wenqin Yu, Wentao Zhang, X. Q. Li, Xiangyue Jin, Xianzu Wang, Xiao Bi, Xiaodong Liu, Xiaohan Wang, Xiaojin Shen, Xiaokang Chen, Xiaokang Zhang, Xiaosha Chen, Xiaotao Nie, Xiaowen Sun, Xiaoxiang Wang, Xin Cheng, Xin Liu, Xin Xie, Xingchao Liu, Xingkai Yu, Xinnan Song, Xinxia Shan, Xinyi Zhou, Xinyu Yang, Xinyuan Li, Xuecheng Su, Xuheng Lin, Y. K. Li, Y. Q. Wang, Y. X. Wei, Y. X. Zhu, Yang Zhang, Yanhong Xu, Yanhong Xu, Yanping Huang, Yao Li, Yao Zhao, Yaofeng Sun, Yaohui Li, Yaohui Wang, Yi Yu, Yi Zheng, Yichao Zhang, Yifan Shi, Yiliang Xiong, Ying He, Ying Tang, Yishi Piao, Yisong Wang, Yixuan Tan, Yiyang Ma, Yiyuan Liu, Yongqiang Guo, Yu Wu, Yuan Ou, Yuchen Zhu, Yudian Wang, Yue Gong, Yuheng Zou, Yujia He, Yukun Zha, Yunfan Xiong, Yunxian Ma, Yuting Yan, Yuxiang Luo, Yuxiang You, Yuxuan Liu, Yuyang Zhou, Z. F. Wu, Z. Z. Ren, Zehui Ren, Zhangli Sha, Zhe Fu, Zhean Xu, Zhen Huang, Zhen Zhang, Zhenda Xie, Zhengyan Zhang, Zhewen Hao, Zhibin Gou, Zhicheng Ma, Zhigang Yan, Zhihong Shao, Zhipeng Xu, Zhiyu Wu, Zhongyu Zhang, Zhuoshu Li, Zihui Gu, Zijia Zhu, Zijun Liu, Zilin Li, Ziwei Xie, Ziyang Song, Ziyi Gao, and Zizheng Pan. Deepseek-v3 technical report, 2025. URL <https://arxiv.org/abs/2412.19437>.
- [5] Venmugil Elango, Nidhi Bhatia, Roger Waleffe, Rasoul Shafipour, Tomer Asida, Abhinav Khattar, Nave Assaf, Maximilian Golub, Joey Guman, Tiyasa Mitra, Ritchie Zhao, Ritika Borkar, Ran Zilberstein, Mostofa Patwary, Mohammad Shoeybi, and Bitan Rouhani. Latentmoe: Toward optimal accuracy per flop and parameter in mixture of experts, 2026. URL <https://arxiv.org/abs/2601.18089>.
- [6] William Fedus, Barret Zoph, and Noam Shazeer. Switch transformers: Scaling to trillion parameter models with simple and efficient sparsity, 2022. URL <https://arxiv.org/abs/2101.03961>.
- [7] Seokjin Go and Divya Mahajan. Moetuner: Optimized mixture of expert serving with balanced expert placement and token routing, 2025. URL <https://arxiv.org/abs/2502.06643>.

- [8] Yu Han, Lehan Pan, Jie Peng, Ziyang Tao, Wuyang Zhang, and Yanyong Zhang. Grace-moe: Grouping and replication with locality-aware routing for efficient distributed moe inference, 2026. URL <https://arxiv.org/abs/2509.25041>.
- [9] Jordan Hoffmann, Sebastian Borgeaud, Arthur Mensch, Elena Buchatskaya, Trevor Cai, Eliza Rutherford, Diego de Las Casas, Lisa Anne Hendricks, Johannes Welbl, Aidan Clark, Tom Hennigan, Eric Noland, Katie Millican, George van den Driessche, Bogdan Damoc, Aurelia Guy, Simon Osindero, Karen Simonyan, Erich Elsen, Jack W. Rae, Oriol Vinyals, and Laurent Sifre. Training compute-optimal large language models, 2022. URL <https://arxiv.org/abs/2203.15556>.
- [10] Connor Holmes, Masahiro Tanaka, Michael Wyatt, Ammar Ahmad Awan, Jeff Rasley, Samyam Rajbhandari, Reza Yazdani Aminabadi, Heyang Qin, Arash Bakhtiari, Lev Kurilenko, and Yuxiong He. Deepspeed-fastgen: High-throughput text generation for llms via mii and deepspeed-inference, 2024. URL <https://arxiv.org/abs/2401.08671>.
- [11] Albert Q. Jiang, Alexandre Sablayrolles, Antoine Roux, Arthur Mensch, Blanche Savary, Chris Bamford, Devendra Singh Chaplot, Diego de las Casas, Emma Bou Hanna, Florian Bressand, Gianna Lengyel, Guillaume Bour, Guillaume Lample, L  lio Renard Lavaud, Lucile Saulnier, Marie-Anne Lachaux, Pierre Stock, Sandeep Subramanian, Sophia Yang, Szymon Antoniak, Teven Le Scao, Th  ophile Gervet, Thibaut Lavril, Thomas Wang, Timoth  e Lacroix, and William El Sayed. Mixtral of experts, 2024. URL <https://arxiv.org/abs/2401.04088>.
- [12] Zewen Jin, Shengnan Wang, Jiaan Zhu, Hongrui Zhan, Youhui Bai, Lin Zhang, Zhenyu Ming, and Cheng Li. Bigmac: A communication-efficient mixture-of-experts model structure for fast training and inference, 2025. URL <https://arxiv.org/abs/2502.16927>.
- [13] Woosuk Kwon, Zhuohan Li, Siyuan Zhuang, Ying Sheng, Lianmin Zheng, Cody Hao Yu, Joseph Gonzalez, Hao Zhang, and Ion Stoica. Efficient memory management for large language model serving with pagedattention. In *Proceedings of the 29th Symposium on Operating Systems Principles, SOSP '23*, page 611–626, New York, NY, USA, 2023. Association for Computing Machinery. ISBN 9798400702297. doi: 10.1145/3600006.3613165. URL <https://doi.org/10.1145/3600006.3613165>.
- [14] Dmitry Lepikhin, HyoukJoong Lee, Yuanzhong Xu, Dehao Chen, Orhan Firat, Yanping Huang, Maxim Krikun, Noam Shazeer, and Zhifeng Chen. Gshard: Scaling giant models with conditional computation and automatic sharding, 2020. URL <https://arxiv.org/abs/2006.16668>.
- [15] Jiamin Li, Yimin Jiang, Yibo Zhu, Cong Wang, and Hong Xu. Accelerating distributed MoE training and inference with lina. In *2023 USENIX Annual Technical Conference (USENIX ATC 23)*, pages 945–959, Boston, MA, July 2023. USENIX Association. ISBN 978-1-939133-35-9. URL <https://www.usenix.org/conference/atc23/presentation/li-jiamin>.
- [16] Yan Li, Zhenyu Zhang, Zhengang Wang, Pengfei chen, and Pengfei Zheng. Semantic parallelism: Redefining efficient moe inference via model-data co-scheduling. In *The Fourteenth International Conference on Learning Representations*, 2026. URL <https://openreview.net/forum?id=MSHP  MpIHZ>.
- [17] Niklas Muennighoff, Luca Soldaini, Dirk Groeneveld, Kyle Lo, Jacob Morrison, Sewon Min, Weijia Shi, Pete Walsh, Oyvind Tafjord, Nathan Lambert, Yuling Gu, Shane Arora, Akshita Bhagia, Dustin Schwenk, David Wadden, Alexander Wettig, Binyuan Hui, Tim Dettmers, Douwe Kiela, Ali Farhadi, Noah A. Smith, Pang Wei Koh, Amanpreet Singh, and Hannaneh Hajishirzi. Olmoe: Open mixture-of-experts language models, 2025. URL <https://arxiv.org/abs/2409.02060>.
- [18] NVIDIA. NVIDIA H100 GPU Datasheet. URL <https://nvdam.widen.net/s/fd11btmmbv/h100-datasheet-2430615>.
- [19] Samyam Rajbhandari, Conglong Li, Zhewei Yao, Minjia Zhang, Reza Yazdani Aminabadi, Ammar Ahmad Awan, Jeff Rasley, and Yuxiong He. DeepSpeed-MoE: Advancing mixture-of-experts inference and training to power next-generation AI scale. In Kamalika Chaudhuri,

- Stefanie Jegelka, Le Song, Csaba Szepesvari, Gang Niu, and Sivan Sabato, editors, *Proceedings of the 39th International Conference on Machine Learning*, volume 162 of *Proceedings of Machine Learning Research*, pages 18332–18346. PMLR, 17–23 Jul 2022. URL <https://proceedings.mlr.press/v162/rajbhandari22a.html>.
- [20] Noam Shazeer, Azalia Mirhoseini, Krzysztof Maziarz, Andy Davis, Quoc V. Le, Geoffrey E. Hinton, and Jeff Dean. Outrageously large neural networks: The sparsely-gated mixture-of-experts layer. *ArXiv*, abs/1701.06538, 2017. URL <https://api.semanticscholar.org/CorpusID:12462234>.
- [21] Siddharth Singh, Olatunji Ruwase, Ammar Ahmad Awan, Samyam Rajbhandari, Yuxiong He, and Abhinav Bhatele. A hybrid tensor-expert-data parallelism approach to optimize mixture-of-experts training. In *Proceedings of the 37th International Conference on Supercomputing, ICS '23*, page 203–214. ACM, June 2023. doi: 10.1145/3577193.3593704. URL <http://dx.doi.org/10.1145/3577193.3593704>.
- [22] Hugo Touvron, Thibaut Lavril, Gautier Izacard, Xavier Martinet, Marie-Anne Lachaux, Timothée Lacroix, Baptiste Rozière, Naman Goyal, Eric Hambro, Faisal Azhar, Aurelien Rodriguez, Armand Joulin, Edouard Grave, and Guillaume Lample. Llama: Open and efficient foundation language models, 2023. URL <https://arxiv.org/abs/2302.13971>.
- [23] Ashish Vaswani, Noam Shazeer, Niki Parmar, Jakob Uszkoreit, Llion Jones, Aidan N. Gomez, Lukasz Kaiser, and Illia Polosukhin. Attention is all you need, 2023. URL <https://arxiv.org/abs/1706.03762>.
- [24] WIKIPEDIA. NVIDIA H100 GPU Datasheet. URL <https://nvdam.widen.net/s/fd11btmmbv/h100-datasheet-2430615>.
- [25] Jinghan Yao, Quentin Anthony, Aamir Shafi, Hari Subramoni, and Dhableswar K. DK Panda. Exploiting inter-layer expert affinity for accelerating mixture-of-experts model inference. In *2024 IEEE International Parallel and Distributed Processing Symposium (IPDPS)*, pages 915–925, 2024. doi: 10.1109/IPDPS57955.2024.00086.
- [26] Shulai Zhang, Ningxin Zheng, Haibin Lin, Ziheng Jiang, Wenlei Bao, Chengquan Jiang, Qi Hou, Weihao Cui, Size Zheng, Li-Wen Chang, Quan Chen, and Xin Liu. Comet: Fine-grained computation-communication overlapping for mixture-of-experts, 2025. URL <https://arxiv.org/abs/2502.19811>.
- [27] Chenggang Zhao, Shangyan Zhou, Liyue Zhang, Chengqi Deng, Zhean Xu, Yuxuan Liu, Kuai Yu, Jiashi Li, and Liang Zhao. DeepEP: an efficient expert-parallel communication library. <https://github.com/deepseek-ai/DeepEP>, 2025.
- [28] Lianmin Zheng, Liangsheng Yin, Zhiqiang Xie, Chuyue Sun, Jeff Huang, Cody Hao Yu, Shiyi Cao, Christos Kozyrakis, Ion Stoica, Joseph E. Gonzalez, Clark Barrett, and Ying Sheng. SGLang: Efficient execution of structured language model programs. In *The Thirty-eighth Annual Conference on Neural Information Processing Systems*, 2024. URL <https://openreview.net/forum?id=VqkAKQibpq>.

A Appendix

A.1 Model Specification

Table 8 lists the architectural dimensions and training hyperparameters used for the small ($\sim 1\text{B}$) and full ($\sim 7\text{B}$) pretraining runs reported in the experiments section. Both models are OLMoE-style transformer MoEs pretrained from scratch on FineWeb-Edu using the OLMoE-1B-7B-0924 tokenizer, with $n_{kv} = 8$ KV heads (matching $H = 8$ expert groups in FoE). During inference, FoE uses a negligible amount of additional GPU memory, due to the increased activation memory from independent residual streams from each expert group.

Variant	Small	Full
<i>Architecture</i>		
Number of Parameters	1.02B	6.85B
Hidden dimension (d)	768	2,048
Number of layers (L)	16	16
Max sequence length	32,768	32,768
Training sequence length	2,048	2,048
Vocabulary	OLMoE-1B-7B-0924 tokenizer	
<i>Attention</i>		
Query heads	8	16
KV heads (n_{kv})	8	8
Head dimension	96	128
RoPE base (θ)	500,000	500,000
RoPE scaling factor	$16\times$	$16\times$
<i>MoE FFN</i>		
Total routed experts (E)	64	64
Top- k experts	8	8
Expert FFN dim multiplier	$1/2$	$1/2$
Expert groups (FoE only, H)	8	8
<i>Training</i>		
Dataset	FineWeb-Edu (train split)	
Local batch size (per DP instance)	16	6
Data-parallel shard size	8	8
Warmup steps	1,000	1,000
Total steps	18,000	50,000
Decay-start step	15,000	40,000
Gradient-norm clip	1.0	1.0
Total tokens trained on	4.7B	4.9B
<i>Optimizer (AdamW)</i>		
Learning rate	6×10^{-4}	6×10^{-4}
Weight decay	0.1	0.1
(β_1, β_2)	(0.9, 0.95)	(0.9, 0.95)
<i>Precision</i>		
Parameter dtype	bfloat16	bfloat16

Table 8: Training configuration for the small ($\sim 1\text{B}$) and full ($\sim 7\text{B}$) FoE and size-matched MoE pretraining runs. Architectural rows that differ between architectures (e.g., expert groups) are marked accordingly; all other settings are shared between the FoE model and its MoE baseline.

A.2 Detailed Communication Traces

To demonstrate the detailed communication patterns during training, we profile communication for a single layer of an 8,192-token batch run on an 8-GPU single node. Figure 5 shows the trace for the standard MoE baseline, whereas Figure 6 illustrates the trace for our FoE architecture. We can observe the significant reduction in synchronization overhead between the two designs. In particular, on our $8\times\text{H100}$ setup we measured a $12.3\times$ reduction in communication time (stream 31).



Figure 5: Detailed communication trace (flamegraph) for a single layer of a standard MoE baseline. Stream 7 is compute and stream 31 is communication.



Figure 6: Detailed communication trace (flamegraph) for a single layer of the proposed FoE architecture. Stream 7 is compute and stream 31 is communication. Note the reduced communication overhead compared to the standard MoE trace in Figure 5.

A.3 End-to-End Forward Pass Latency

Table 9 illustrates the end-to-end forward-pass latency as the synthetic batch size increases. In standard MoE parallelism, synchronization requires global dispatch across the network topology. As synthetic batch sizes expand beyond 2048, the total forward pass latency escalates substantially, bottlenecked by the all-to-all communication overhead. By contrast, FoE confines routing and load balancing within localized expert groups, keeping forward-pass latency near-constant up to moderately large batch sizes and scaling smoothly thereafter, yielding up to a $5.2\times$ speedup at a synthetic batch size of 24,576.

Batch Size	Mixture of Experts (s)	Federation of Experts (s)	Speedup (MoE / FoE)
1	0.06106	0.05849	1.04 \times
2	0.06646	0.06644	1.00 \times
8	0.06878	0.07161	0.96 \times
128	0.06886	0.06831	1.01 \times
512	0.07545	0.07782	0.97 \times
1,024	0.07485	0.08095	0.92 \times
2,048	0.08855	0.06826	1.30 \times
4,096	0.16541	0.07569	2.19 \times
8,192	0.46442	0.12948	3.59 \times
12,288	0.97771	0.21813	4.48 \times
16,384	1.64213	0.33635	4.88 \times
20,480	2.49477	0.48566	5.14 \times
24,576	3.48559	0.66934	5.21 \times

Table 9: End-to-end forward-pass latency (seconds) measured across synthetic batch sizes.